"Living" Free Radical Polymerization in Tubular Reactors. I. Modeling of the Complete Molecular Weight Distribution Using Probability Generating Functions

Mariano Asteasuain,* Matheus Soares, Marcelo K. Lenzi, Michael Cunningham, Claudia Sarmoria, José Carlos Pinto, Adriana Brandolin

This is the first of a series of works aiming at developing a tool for designing "living" free radical polymerization processes in tubular reactors, in order to achieve tailor-made MWDs. A mathematical model of the nitroxide-mediated controlled free radical polymerization is built and implemented to predict the complete MWD. It is shown that this objective may be achieved accurately and efficiently by means of the probability generating function (pgf) transformation. Comparison with experimental data is good. The potential of the resulting model for optimization activities involving the complete MWD is also shown.

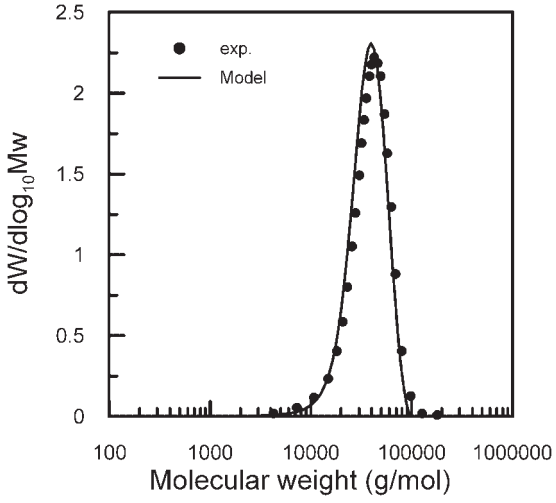

M. Asteasuain, C. Sarmoria, A. Brandolin
Planta Piloto de Ingeniería Química, PLAPIQUI (UNS–CONICET), Camino La Carrindanga Km 7, 8000 Bahía Blanca, Argentina
Fax: +54 291 486 1600; E-mail: masteasuain@plapiqui.edu.ar
M. Soares, J. C. Pinto
Programa de Engenharia Química/COPPE, Universidade Federal do Rio de Janeiro, Cidade Universitária, CP: 68502, Rio de Janeiro 21945-970, RJ, Brazil
M. K. Lenzi
Departamento de Engenharia Química, Universidade Federal do Paraná, Setor de Tecnologia, Jardim das Américas, CP: 19011, Curitiba 81531-990, PR, Brazil
M. Cunningham
Department of Chemical Engineering, Queen's University, Dupuis Hall, 19 Division Street, Kingston, ON K7L 3N6, Canada

Introduction

The production of polymer resins with controlled molecular structure is of great interest in the field of polymeric materials. Resins with controlled molecular structure are usually produced through living or functional polymerizations, and generally present narrow molecular weight distributions (MWD) and either block or alternating monomer composition distributions in the case of copolymers. However, conventional living polymerizations, like anionic polymerization, present inconveniencies such as a very high sensitivity to impurities, which limit industrial applications. In this context, in the last few decades,

Macromol. React. Eng. **2007**, *1*, 622–634

DOI: 10.1002/mren.200700026

"living" (or controlled) free radical polymerizations were developed. They combine advantages of both living polymerization and free radical polymerization. Their kinetic behavior shares some similarities to traditional living polymerization, allowing for more detailed control of the structure of the polymer chains. At the same time, they are capable of polymerizing a larger number of monomers and tolerating a greater concentration of impurities, like conventional free radical polymerization.[1] There are several variants on controlled free radical polymerization. The most common are atom-transfer radical polymerization (ATRP), reversible addition–fragmentation chain transfer (RAFT), and living radical polymerization mediated by nitroxides (NMP).[2,3] A detailed discussion may be found elsewhere.[2–5] Briefly, in these polymerizations growing radicals are subject to reversible termination or reversible transfer reactions, alternating relatively long "dormant" periods of inactivity with short periods of normal activity. A dynamic equilibrium is established between a small number of growing radicals and a large quantity of inactive chains. The type of inactive chain varies with the particular type of polymerization. For example, in ATRP they are alkyl halides, in RAFT they are thioesters, and in NMP they are alkoxyamines.[3] The generation of free radicals proceeds by different routes in each type of polymerization: catalytic reaction in ATRP, degenerative exchange with inactive species in RAFT, or thermal initiation in NMP.[3]

Due to the mentioned equilibrium reaction between active and inactive molecules all polymer chains grow at almost the same rate, resulting in low polydispersity indexes. Excellent examples of this feature may be found in the experimental database reported by Roa-Luna et al.[6] on conversion, number-average molecular weight, and polydispersity index for NMP. On the other hand, experimental work has been reported in which NMP is used in combination with conventional free radical polymerization to produce bimodal distributions in batch reactors.[7] Moreover, theoretical studies have shown that it is also possible to use exclusively living free radical polymerization to obtain distributions with more complex shapes and multimodal behavior, through proper manipulation of the operating conditions or the reactor configuration.[8]

A mathematical model able to predict the complete MWD is an essential tool to study the influence of the different operating variables on the final molecular properties, and, ultimately, to design the operating conditions for producing a polymer with tailor-made MWD. Detailed analysis on previous modeling efforts may be found elsewhere.[1,8–14] Most models[1,8,13–17] deal with the prediction of conversion and average molecular weights. Only few reported models of this process include the prediction of the complete MWD.[8–12] In some of them, this task is performed by assuming a priori the shape of the distribution, such as a Schulz distribution.[8] Although this methodology can be applied in the simple case of monomodal narrow distributions, it cannot be used in the case of more complex shapes, like bimodal distributions. Other models calculate the MWD using techniques that are computationally expensive, such as Monte Carlo simulations[10] or by solving the mass balances of all polymeric chains composing the MWD.[11] The commercial software PREDICI®, which uses the h-p Galerkin method to compute the MWD[18] has also been employed to model RAFT processes.[9,12] However, as far as we know this method has not been applied in optimization problems.

A recently developed methodology for modeling the complete MWD in free radical polymerization processes uses the probability generating function (pgf) transformation.[19–21] This approach does not assume a priori any particular shape for the MWD, which allows it to be applied in a broader set of polymerization problems. Besides, each point in the MWD may be calculated independently from the others, which allows to freely modify the number of such points to be predicted without any loss in accuracy. Therefore, the size of the mathematical model, which depends directly on the number of calculated points in the MWD, can be tailored for different problems according to the required level of detail on the MWD.

This is the first of a series of works with the final objective of developing a tool to aid in designing controlled free radical polymerization processes in order to achieve tailor-made MWDs. Here we present a mathematical model of the nitroxide-mediated living free radical polymerization taking place in a tubular reactor that applies the pgf technique to calculate the complete MWD. In order to show the appropriateness of the pgf technique for simulation and optimization activities involving the complete MWD, its accuracy and computational efficiency are analyzed.

Mathematical Model

In nitroxide-mediated living free radical polymerizations, nitroxide radicals reversibly cap the growing radicals to form dormant species. Polymerization of styrene using 2,2,6,6-tetramethylpiperidinyl-1-oxy (TEMPO) as capping agent is considered in this work. The kinetic mechanism considered in this model is shown in Equation (1)–(9). It is based on the ones employed by Zhang and Ray[1] and Lenzi.[11]

Initiation

$$I \xrightarrow{k_d} 2R_i \tag{1}$$

$$R_i + M \xrightarrow{\text{efic.}k_i} R_1 \tag{2}$$

Monomer thermal initiation

$$3M \xrightarrow{k_{th}} R_1 + R_2 \quad (3)$$

Capping and uncapping reactions

$$X + R_n \xrightarrow{k_{cap}} D_n \quad (4)$$

$$D_n \xrightarrow{k_{uncap}} R_n + X \quad (5)$$

Propagation

$$R_n + M \xrightarrow{k_p} R_{n+1} \quad (6)$$

Transfer to monomer

$$R_n + M \xrightarrow{k_{trm}} R_1 + P_n \quad (7)$$

Termination by combination

$$R_n + R_m \xrightarrow{k_t} P_{n+m} \quad (8)$$

Disproportionation involving nitroxide

$$D_n \xrightarrow{k_{disp1}} P_n + Y \quad (9)$$

Initiation, propagation, transfer, and termination reactions are common to most free radical polymerizations. The reversible reaction between growing macroradicals and dormant polymer [Equation (4) and (5)] controls the growth rate of polymer chains and gives the living property to the free radical polymerization. Termination by disproportionation and disproportionation of deactivated TEMPO, two reactions considered by Lenzi,[11] were not incorporated because they had a negligible effect on monomer conversion and polymer molecular properties for the operating conditions considered in this work. This was verified by comparing model outputs on conversion and MWD with and without these reactions, for representative sets of operating conditions. The kinetic parameters for the mentioned reactions were those reported by Ma et al.,[22] while those for the remaining reactions were the ones reported in Table 1. Model predictions showed no noticeable differences. The only disparities appeared in nonsignificant digits.

The mathematical model is built up from the mass balances for the different species present in the reaction. The complete set of mass balances is shown in Table 2. These equations correspond to a plug flow tubular reactor with variable reaction mixture density and axial velocity. Although flow distortions can actually be present, previous works[23,24] have shown that the plug flow assumption yields reasonable results for the operating conditions considered in this work. This was attributed to the fact that the average values of the properties did not differ significantly between a plug flow model and models with different velocity profiles, because of the averaging of the results provided by the different stream lines. The good agreement of model results with experimental data that will be presented later supports this point. Uniform reactor temperature is considered, so the energy balance was not included. This temperature profile can actually be achieved very efficiently with the control system included in the experimental setup employed in this work, as described in detail in previous experimental and modeling studies.[23,24] The laboratory scale reactor dimensions aid in achieving the isothermal operation in spite of the exothermic

Table 1. Kinetic constants, model parameters, and density equations for monomer, polymer and reaction mixture.

$k_d/\text{min}^{-1} = 1.02 \times 10^{17} e^{\left(-\frac{30000}{1.987T}\right)}$ a)	$\rho_{St}/(g \cdot L^{-1}) = 0.919 \times 10^3 - 6.65 \times 10^{-1} T/^\circ C$ a)
$k_{th}/(L^2 \cdot mol^{-2} \cdot min^{-1}) = 1.314 \times 10^7 e^{\left(-\frac{27440.47}{1.987T}\right)}$ a)	$\rho_{pol}/(g \cdot L^{-1}) = 0.993 \times 10^3 - 2.65 \times 10^{-1} T/^\circ C$ a)
$k_{cap}/(L \cdot mol^{-1} \cdot min^{-1}) = 3.018 \times 10^{11} e^{\left(-\frac{3722}{1.987T}\right)}$ a)	$\rho_{mix} = \frac{1}{\frac{x_{St}}{\rho_{St}} + \frac{1-x_{St}}{\rho_{pol}}}$
$k_{uncap}/(min^{-1}) = 1.2 \times 10^{15} e^{\left(-\frac{29683}{1.987T}\right)}$ a)	$x_{St} = \frac{C_M M_{St}}{\rho_{mix}}$
$k_p/(L \cdot mol^{-1} \cdot min^{-1}) = 2.5596 \times 10^9 e^{\left(-\frac{7769.17}{1.987T}\right)}$ a)	$M_{St}/(g \cdot mol^{-1}) = 104.14$
$k_{trm}/(L \cdot mol^{-1} \cdot min^{-1}) = k_p 13.188\, e^{\left(-\frac{2820}{T}\right)}$ a)	$M_{BPO}/(g \cdot mol^{-1}) = 243.23$
$k_t/(L \cdot mol^{-1} \cdot min^{-1}) = k_p^2 \times 1.83 \times 10^{-7} e^{\left(\frac{12452.2}{1.987T}\right)}$ a)	$M_{TEMPO}/(g \cdot mol^{-1}) = 156.38$
$k_{disp1}/(min^{-1}) = 3.42 \times 10^{16} e^{\left(-\frac{36566.15}{1.987T}\right)}$ b)	Reactor diameter/dm = 0.0635
$f = 0.62$	Reactor diameter/dm = 63

a)Zhang and Ray;[1] b)Ma et al.[22]

Macromol. React. Eng. **2007**, *1*, 622–634

Macromolecular Journals

DOI: 10.1002/mren.200700026

Table 2. Mass balance equations.

Global mass balance

$$\frac{d(\rho_{mix} v)}{dz} = 0 \quad (10)$$

Individual balance of entity j

$$\frac{d(C_j v)}{dz} = r_j \quad (11)$$

Initiator

$$r_I = -k_d C_I \quad (12)$$

Monomer

$$r_M = -k_p C_M C_{\lambda_0} - k_{trm} C_M C_{\lambda_0} - 3k_{th} C_M^3 \quad (13)$$

TEMPO

$$r_X = k_{uncap} C_{\mu_0} - k_{cap} C_X C_{\lambda_0} \quad (14)$$

Macroradical of chain length n ($n = 1,\ldots,\infty$)

$$r_{R_n} = 2efic\, k_d C_I \delta_{n,1} + k_p C_M C_{R_{n-1}}(1-\delta_{n,1}) - k_p C_M C_{R_n} - k_t C_{R_n} \sum_{n=1}^{\infty} C_{R_n} - k_{trm} C_M C_{R_n} + k_{uncap} C_{D_n} - k_{cap} C_X C_{R_n} + (\delta_{n,1} + \delta_{n,2}) k_{th} C_M^3 \quad (15)$$

Dormant polymer of chain length n ($n = 1,\ldots,\infty$)

$$r_{D_n} = -k_{uncap} C_{D_n} + k_{cap} C_X C_{R_n} - k_{disp1} C_{D_n} \quad (16)$$

Dead polymer of chain length n ($n = 1,\ldots,\infty$)

$$r_{P_n} = k_{trm} C_M C_{R_n} + \frac{k_t}{2} \sum_{m=1}^{n-1} C_{R_m} C_{R_{n-m}} + k_{disp1} C_{D_n} \quad (17)$$

reaction. However, the energy balance can effortlessly be incorporated if needed. Values of the kinetic constants, model parameters, and expressions for the monomer, polymer, and the reaction mixture densities are presented in Table 1. Gel effect was not included in the model because the case studies to which it is applied involve low conversions, for which this effect is not significant even in conventional bulk free radical polymerization. Furthermore, the gel effect is less important in nitroxide-mediated living free radical polymerization, where bimolecular termination reactions are fewer than in a conventional free radical polymerization.[25] Thermodynamic modeling and phase equilibrium calculations were not included, as it is assumed that the reaction occurs only in liquid media.

It is important to mention that the kinetic mechanism and model parameters employed in this work are considered to be reliable, since they were successfully used to predict experimental data, obtained in batch reactors, of monomer conversion, average molecular weights,[1,11] and also full MWDs obtained by direct integration of mass balances.[11] Moreover, it was possible to predict complex distributions obtained using a sequence of living and conventional free radical polymerizations in batch reactors.[11] In this case the kinetic model was solved in combination with a model for conventional radical polymerization.

The well-known moment technique is used to calculate the number and weight-average molecular weights. Balance equations are set up for the first three moments of the chain length distributions of the macroradicals, dormant polymer, and dead polymer, which are shown in Table 3. These moments are used to calculate the average molecular weights according to Equation (21) and (22) in Table 3. The reaction terms in the balance equations are consistent with the ones reported by Lenzi[11] for a batch reactor.

Table 3. Moments, average molecular weights and conversion equations.

ath order moment of the chain length distribution of macroradicals ($a = 0, 1, 2$)

$$r_{\lambda_a} = 2efic\, k_d C_I + k_p C_M \sum_{j=0}^{a} \binom{a}{j} C_{\lambda_j} - k_p C_M C_{\lambda_a} - k_t C_{\lambda_0} C_{\lambda_a} - k_{trm} C_M C_{\lambda_a} + k_{uncap} C_{\mu_a} - k_{cap} C_X C_{\lambda_a} + (1 + 2^a) k_{th} C_M^3 \quad (18)$$

ath order moment of the chain length distribution of the dormant polymer ($a = 0, 1, 2$)

$$r_{\mu_a} = -k_{uncap} C_{\mu_a} + k_{cap} C_X C_{\lambda_a} - k_{disp1} C_{\mu_a} \quad (19)$$

ath order moment of the chain length distribution of the dead polymer ($a = 0, 1, 2$)

$$r_{\xi_a} = k_{trm} C_M C_{\lambda_a} + \frac{k_t}{2} \sum_{j=0}^{a} \binom{a}{j} C_{\lambda_j} C_{\lambda_{a-j}} + k_{disp1} C_{\mu_a} \quad (20)$$

Number-average molecular weight

$$\overline{M}_n = M_{St} \frac{C_{\lambda_1} + C_{\mu_1} + C_{\xi_1}}{C_{\lambda_0} + C_{\mu_0} + C_{\xi_0}} \quad (21)$$

Weight average molecular weight

$$\overline{M}_w = M_{St} \frac{C_{\lambda_2} + C_{\mu_2} + C_{\xi_2}}{C_{\lambda_1} + C_{\mu_1} + C_{\xi_1}} \quad (22)$$

Polydispersity index

$$PDI = \frac{\overline{M}_w}{\overline{M}_n} \quad (23)$$

Monomer conversion

$$conv = \frac{C_{\lambda_1} + C_{\mu_1} + C_{\xi_1}}{C_{\lambda_1} + C_{\mu_1} + C_{\xi_1} + C_M} \quad (24)$$

Modeling of the Complete MWD

Modeling the MWD implies determining the amount of polymer molecules of every possible chain length. In general, setting up the mass balances for these species leads to an infinite number of equations because the chain length can take any value between 1 and infinity, and the equations for the different chain length values are generally interdependent. However, a finite number of equations can be obtained for polymerization systems in which the mass balance for a polymer molecule of chain length n depends only on the concentrations of polymer molecules of chain lengths less than or equal to n. This is the case of the living free radical polymerizations described by a kinetic mechanism like the one shown in Equation (1)–(9). Therefore, the MWD can be obtained directly from the mass balances of the macromolecules. Nevertheless, balance equations have to be solved for all values between 1 and a given chain length n_{max} that may take values of several orders of magnitude to cover the significant portion of the distribution curve. This approach has been employed by Lenzi[11] for calculating the complete MWD in a batch reactor model of the nitroxide-mediated styrene living free radical polymerization.

In this work a different methodology is applied for modeling the complete MWD. It is based on a transformation of the mass balances of the polymeric species by means of pgfs.[19–21] pgf transformation is applied to the infinite set of mass balance equations, leading to a finite set of equations where the dependent variable is the pgf transform of the MWD. The pgfs calculated by solving the transformed equations, are then inverted to recover the MWD. pgfs are defined for each type of macromolecule as shown in Equation (25)–(27).

$$\phi_a(l) = \sum_{n=1}^{\infty} l^n \frac{n^a C_{R_n}}{C_{\lambda_a}} \tag{25}$$

$$\varphi_a(l) = \sum_{n=1}^{\infty} l^n \frac{n^a C_{D_n}}{C_{\mu_a}} \tag{26}$$

$$\psi_a(l) = \sum_{n=1}^{\infty} l^n \frac{n^a C_{P_n}}{C_{\zeta_a}} \tag{27}$$

In the above equations subscript a identifies the type of MWD being transformed. The MWD expressed as number fraction versus molecular weight, weight fraction versus molecular weight or the product of weight fraction times the molecular weight versus molecular weight corresponds to $a = 0$, 1, or 2, respectively. These distributions are

Table 4. pgfs and Stehfest inversion algorithm equations.

pgfs of the chain length distribution of macroradicals ($a = 0$, 1, 2)

$$r_{(\lambda_a\phi_a(l))} = 2\text{efick}_d C_I + k_p C_M l \sum_{j=0}^{a} \binom{a}{j} C_{(\phi_j(z)\lambda_j)} - k_p C_M C_{(\phi_a(l)\lambda_a)} - k_t C_{\lambda_0} C_{(\phi_a(l)\lambda_a)} - k_{trm} C_M C_{(\phi_a(l)\lambda_a)} + k_{uncap} C_{(\mu_a\varphi_a(l))} - k_{cap} C_X C_{(\phi_a(l)\lambda_a)} + (l + l^2 2^a) k_{th} C_M^3 \tag{28}$$

pgfs of the chain length distribution of the dormant polymer ($a = 0$, 1, 2)

$$r_{(\mu_{a,}\varphi_{a,}(l))} = -k_{uncap} C_{(\mu_{a,}\varphi_{a,}(l))} + k_{cap} C_X C_{(\lambda_{a,}\varphi_{a,}(l))} - k_{disp1} C_{(\mu_{a,}\varphi_{a,}(l))} \tag{29}$$

pgfs of the chain length distribution of the dead polymer ($a = 0$, 1, 2)

$$r_{(\xi_a\psi_a(l))} = k_{trm} C_M C_{(\lambda_a\phi_a(l))} + \frac{k_t}{2} \sum_{j=0}^{a} \binom{a}{j} C_{(\lambda_j\phi_j(l))} C_{(\lambda_{a-j}\phi_{a-j}(l))} + k_{disp1} C_{(\mu_a\varphi_a(l))} \tag{30}$$

pgfs of the overall polymer ($R_n + D_n + P_n$)

$$\vartheta_a(l) = \frac{\lambda_a\phi_a(l) + \mu_a\varphi_a(l) + \zeta_a\psi_a(l)}{\lambda_a + \mu_a + \zeta_a} \tag{31}$$

Stehfest inversion algorithm

$$p_a(n) = \frac{\ln(2)}{n} \sum_{j=1}^{J} K_J \vartheta_a[\exp(-j\ln(2)/n)]$$
$$K_j = (-1)^{j+J/2} \sum_{k=[(j+1)/2]}^{\min(jJ/2)} \frac{k^{J/2}(2k)!}{(J/2-k)!k!(k-1)!(j-k)!(2k=j)!} \tag{32}$$

where $p_a(n)$ is the number, weight, or chromatographic distribution of the overall polymer for $a = 0$, 1, or 2, respectively.

Macromol. React. Eng. **2007**, *1*, 622–634

Macromolecular Journals
DOI: 10.1002/mren.200700026

also known as number, weight, or chromatographic MWD. The resulting transformed equations are shown in Table 4 [Equation (28)–(30)]. The same subscript a is used to identify the order of the moments and the type of MWD represented by the pgf transform, because specific moments and distribution types are coupled in the pgf equations, as can be seen in Table 4 [i.e., number distribution transform ($a=0$) and zero order moment ($a=0$), weight distribution transform ($a=1$) and first order moment ($a=1$)]. The pgf of the MWD of the overall polymer can be obtained from the pgfs of the distributions of the individual polymeric species as shown by Equation (31). The inversion algorithm is composed of a set of algebraic equations that are solved together with the pgf equations and allow for the recovery of the MWDs from their corresponding pgf transforms. In this work we apply the Stehfest inversion algorithm,[19–21] corresponding to Equation (32) in Table 4.

The pgf method allows for calculation of any point of the MWD independently of any other. The result is always the same for any given point, regardless of how many other points for the same distribution are calculated. This is useful because often a small number of points is enough for a good description of the shape of the MWD. In consequence, the size of the model and therefore the computational time can be adjusted according to different requirements. For the Stehfest inversion method, the number of differential equations involved in the MWD prediction is as follows:

$$n_{eq} = J n_{point} n_{spc} n_{dist} \tag{33}$$

where J is a parameter of the Stehfest method [see Equation (32) in Table 4], n_{points} is the number of calculated points of the MWD, n_{spc} is the number of different polymeric species for which the pgf transforms are calculated, and n_{dist} is the number of "types" of calculated distributions (for example: $n_{dist}=1$: number distribution, $n_{dist}=2$: number and weight distributions). For the cases solved here, the value of J was 12, n_{spc} was 3 (radicals, dormant polymer, and dead polymer) and n_{dist} was 2. The same value for parameter J was used for all the cases. In general, a low value of J results in a poor inversion of the pgf because too few terms are used in the inversion formula. Ideally, the value of J should be infinity. However, a very high value incorporates numerical noise due to error propagation. The right choice depends on the precision of the calculated pgfs, which in turn depends on the DAE system and the numerical solver. Useful guidelines for selecting a good value for this parameter can be found elsewhere.[26] Notice that the values of the dummy variable l for which Equation (28)–(31) have to be formulated are determined by the arguments of ϑ_a in Equation (32). On the other hand, Equation (15)–(17) must be solved for n ranging from 1 to n_{max} when the direct integration of the mass balances is employed for purposes of comparison with the pgf method.

The pgf method is a general approach, which has no inherent restrictions limiting the polymeric systems it can be applied to. Up to now, the pgf method has been successfully employed for modeling the MWD in different free radical polymerization systems in the pregel region, including nonisothermal operation, complex kinetic mechanisms, and branched polymers. Some of these are: peroxide modification of polyethylene[27] and poly(propylene),[28] styrene polymerization with bifunctional initiators,[29] and high pressure ethylene polymerization in tubular reactors.[30]

The mathematical model was implemented in the commercial software gPROMS (Process Systems Enterprise, Ltd.).[31] A DAE solver that is based on variable time step/variable order backward differentiation formulae (BDF) is used for the integration of the model equations. For the specific task of computing the coefficients of the Stehfest algorithm [coefficients K_j in Equation (32)], which involve quotients of large factorials with alternating signs, a procedure was developed in FORTRAN. This code has special built-in functions for calculating the factorials. The FORTRAN procedure was linked to the main gPROMS model using the Foreign Object interface of this software.

Obtaining Target MWDs

An optimization problem is formulated here to characterize the performance of the proposed pgf technique, when compared to the performance of the direct integration of the mass balances. For this reason, solution of complex optimization problems is not pursued at this stage. It is assumed that one is interested in producing given MWDs through living free-radical polymerizations, where the target distributions span different molecular weight ranges. This may be regarded as a useful numerical test problem, that shows that the pgf approach is efficient and suitable for future implementation of more demanding optimization tasks such as obtaining multimodal MWDs for which this type of polymerization shows potential.

For each target distribution the mathematical formulation of the optimization problem is

$$\begin{aligned} &\min_{f_{St}, f_{BPO}, f_{TEMPO}, T} FO = \sum_i \left(1 - \frac{w(n_i)}{w_{target}(n_i)}\right)^2 \\ &st \\ &\text{process model} \\ &f_{St,min} \le f_{St} \le f_{St,max} \\ &f_{BPO,min} \le f_{BPO} \le f_{BPO,max} \\ &f_{TEMPO,min} \le f_{TEMPO} \le f_{TEMPO,max} \\ &T_{min} \le T \le T_{max} \end{aligned} \tag{34}$$

where "process model" involves Equation (10)–(14), (18)–(24), (28)–(32), and kinetic constants, densities, and styrene mass fraction equations shown in Table 1, $w(n_i)$ and $w_{target}(n_i)$ are the predicted and desired values, respectively, of the weight fraction of the overall polymer of chain length n_i; f_{St}, f_{BPO}, and f_{TEMPO} are the flow rates of styrene, BPO, and TEMPO, respectively, and T is the reactor temperature. Therefore, it is desired to produce a certain MWD through manipulation of feed flow rates and reactor temperature, which are subject to real operation constraints. This is a very realistic scenario for the operation of tubular reactors, as feed flow rates and temperatures can be easily manipulated at plant site.

In each case the optimization problem was solved by calculating the MWD with the pgf technique and with the direct integration of the mass balances, for the same starting point and optimization solver parameters. The software gPROMS was used for this task. The employed optimization solver integrates the DAE system at each iteration of the optimization algorithm. A DAE solver that is based on variable time step/variable order BDF is used for the integration of the model DAE system and its sensitivity equations at each iteration. This provides with information on the final values of the objective function and constraints, and their gradients with respect to the optimization variables. This information is then used by a nonlinear programming (NLP) solver to adjust the values of the optimization variables. A sequential quadratic programming method is used for this task. The optimization solver implements a single shooting algorithm, which means that a single integration of the dynamic model over the entire horizon is performed for each evaluation of the objective function.[31]

In the following section, validity of the model and its potential for optimization activities are analyzed. First, model calculations are compared with experimental data. Then, it is shown that MWDs calculated with the pgf technique are the same as the ones obtained by direct integration of the mass balances. It is also shown that the same level of accuracy is obtained with the pgf in a shorter CPU time. Finally, two examples of MWD tailoring are also included, illustrating the efficiency of the pgf technique for optimization problems.

Results and Discussion

In order to assess the validity of the tubular reactor model, its predictions were compared against experimental data on NMP of styrene, both from the literature[6,32–34] and from our laboratories. First, average molecular weights obtained by processing the MWDs predicted with the tubular reactor model are compared with independent experimental results on average molecular weights. These data were obtained in a tubular reactor and in a batch reactor. The setup for the batch experiment is described in the work by Lenzi.[11] The tubular reactor configuration is the same described elsewhere[23,24] for another polymerization system except for the reactor dimensions. The actual dimensions used in the experiments reported in this work are shown in Table 1. The experimental device includes an insulating jacket surrounding the reactor, whose temperature is regulated by a PID controller monitoring the reactor temperature along the axial distance. This allows achieving the desired uniform reactor temperature. For the process conditions considered in this work, the reactor operates with a Reynolds number of approximately 20, and a high Peclet number.[35] The pressure drops in the reactor were below 20%.

The molecular weight averages were calculated from the predicted MWDs as shown in Equation (35) and (36).

$$\overline{M}_n = M_{St} \sum_{i=1}^{n_{max}} i\, n(i) \tag{35}$$

$$\overline{M}_w = M_{St} \sum_{i=1}^{n_{max}} i\, w(i) \tag{36}$$

In order to provide a suitable basis for the comparison with the batch reactor, the average molecular weight profiles corresponding to the tubular reactor are calculated as a function of the reactor residence time (τ), which depends on the axial distance as indicated by Equation (37).

$$\frac{d\tau}{dz} = \frac{1}{v}, \tau(0) = 0 \tag{37}$$

The comparison between the average molecular weights calculated from the predicted MWDs and the experimental data is shown in Figure 1 together with the operating conditions. Experimental information from the tubular reactor was only available at the reactor exit. Therefore, in order to test the profiles predicted by the model, data from the same reaction carried out in a batch reactor at equivalent operating conditions are also included.

The tubular reactor model also calculates the average molecular weights by the well-known method of moments [Equation (21) and (22)], without making use of the calculated MWDs. A comparison between the values of $\overline{M}_n$ and $\overline{M}_w$ calculated by the method of moments and those obtained from the predicted MWDs are also presented in Figure 1. It can be seen that there is an excellent agreement between the average molecular weights calculated from the predicted MWDs and from the method of moments, as well as with the experimental data.

Macromolecular Journals
DOI: 10.1002/mren.200700026

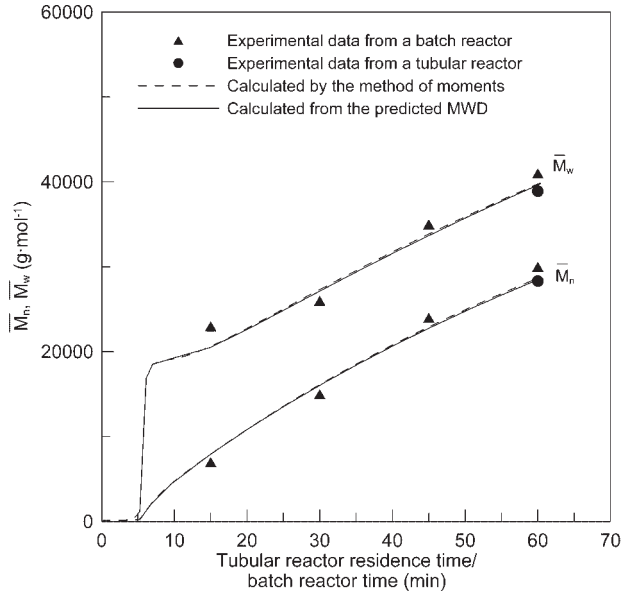

Figure 1. Experimental and calculated average molecular weights. Operating conditions: $T = 133\ ^\circ C$; inlet (tubular reactor) or initial (batch reactor) mass fractions: $x_{St} = 0.9976$, $x_{BPO} = 0.00134$, $x_{TEMPO} = 0.00106$; $f_{Tot} = 3\ g \cdot min^{-1}$ (tubular reactor).

In order to further validate the model, batch data from the literature[6,32–34] were used. As initiator efficiency has been reported to change with [TEMPO]/[BPO] ratios,[1] values of 0.54 and 0.62 were used for the low and high [TEMPO]/[BPO] ratios. Results are shown in Figure 2 and 3 for conversion and polydispersity index, respectively. Model predictions agree well with the experimental data. The level of agreement is comparable to that reported for previously published models.[1,14] It may be seen in Figure 2 that model predictions are good even at high conversions, although the gel effect was not included in the model.

MWD prediction by the tubular reactor model is also compared with an experimental MWD[34] produced in a batch reaction, as shown in Figure 4. The model is able to appropriately predict the MWD produced by reacting styrene with benzoyl peroxide and TEMPO.

In what follows, the accuracy and efficiency of the pgf technique is analyzed. Figure 5 and 6 show simulation results for the MWD expressed in number and weight fractions calculated with the pgf technique and by direct integration of the mass balances. The operating conditions of the tubular reactor are shown in Figure 5. It can be seen that the MWDs calculated with the pgf technique coincide with the ones calculated by direct integration of the mass balances. However, the CPU time required to perform the simulation when using the pgf technique is shorter. The reason is that the number of differential equations in the pgf model is considerably smaller. With the direct integration of the mass balances, balances for the three macromolecular species [Equation (15)–(17)] for all chain

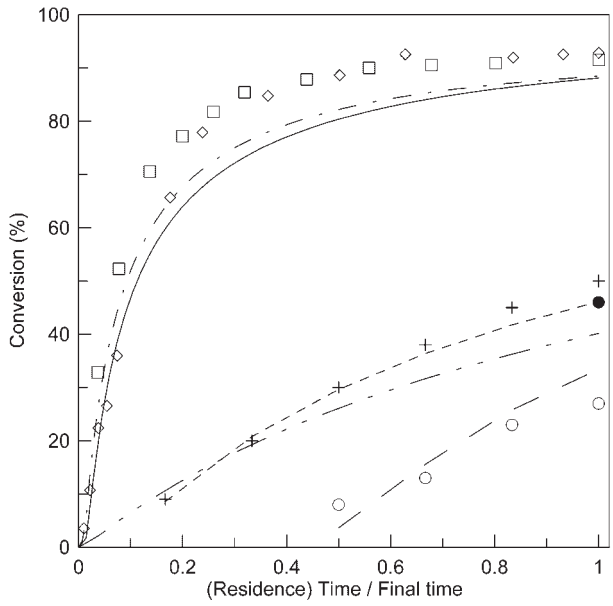

Figure 2. Conversion vs. time. (a) — model ◇ exp.[6] ($T = 120\ ^\circ C$, $x_{St,o} = 0.984$, $x_{BPO,o} = 0.010$ [TEMPO]/[BPO] = 1.1), (b) — - — model □ exp.[6] ($T = 130\ ^\circ C$, $x_{St,o} = 0.984$, $x_{BPO,o} = 0.010$ [TEMPO]/[BPO] = 1.1), (c) - - - model + exp.[32,33] ($T = 125\ ^\circ C$, $x_{St,o} = 0.984$, $x_{BPO,o} = 0.010$ [TEMPO]/[BPO] = 1.1), (d) — — model ○ exp.[32,33] ($T = 125\ ^\circ C$, $x_{St,o} = 0.984$, $x_{BPO,o} = 0.010$ [TEMPO]/[BPO] = 1.3), (e) — - — model ● exp.[34] ($T = 125\ ^\circ C$, $x_{St,o} = 0.9953$, $x_{BPO,o} = 0.0002$ [TEMPO]/[BPO] = 1.25).

lengths values between 1 and n_{max} must be solved. In the example $n_{max} = 1\,000$ was used for an appropriate description of the MWD. When using the pgf technique, the number of equations is proportional to the number of calculated points of the MWD. In the example, 30 points of

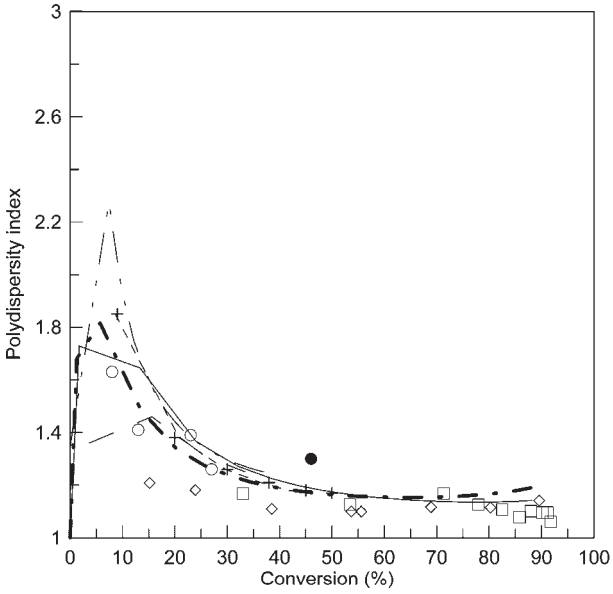

Figure 3. Polydispersity index versus conversion. Symbols and lines: see Figure 2.

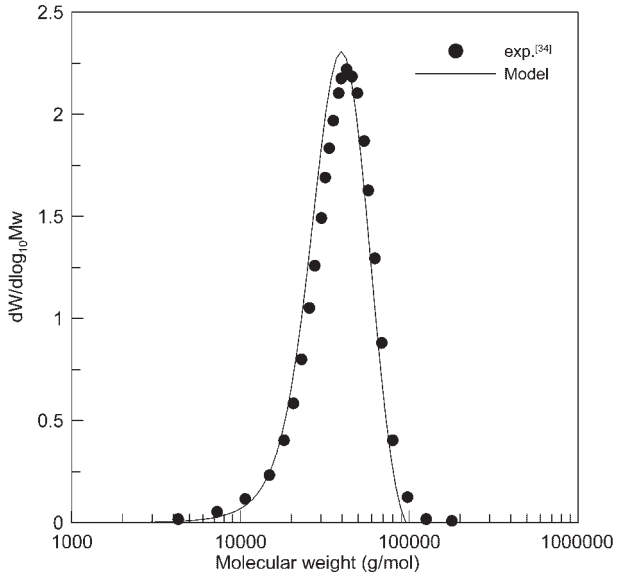

Figure 4. MWD. Operating conditions: $T = 125\ ^{\circ}C$, $x_{St,o} = 0.9953$, $x_{BPO,o} = 0.0002$, [TEMPO]/[BPO] = 1.25, (residence) time = 255 min.

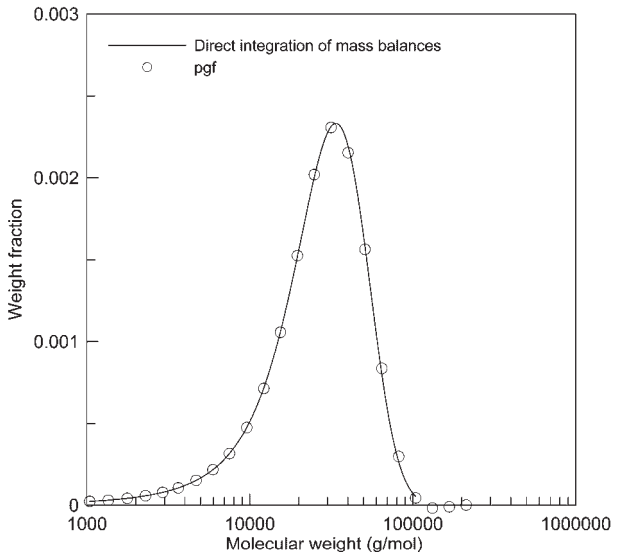

Figure 6. Weight fraction of the overall polymer calculated with the pgf technique and by direct integration of the mass balances. Operating conditions: see Figure 5.

the distributions were computed, and it can be seen that they give a suitable representation of the MWD. Under these conditions, the number of differential equations was approximately 3 000 for the direct integration of the mass balances, and 2 000 for the pgf technique [see Equation (33)].

The corresponding CPU times in a personal computer with a Pentium IV processor of 3 GHz and 1 GB RAM were 90 and 13 s, respectively. The efficiency of the pgf technique increases as the required level of detail of the MWD diminishes. For instance, assuming that only a rough description of the curve was needed, only six points of the previous distribution were calculated. As explained above, since the calculation of each point on the curve is independent of any other point, all six of them fell on the same curve as the 30 points in Figure 6. In this case, the number of differential equations was reduced to about 400 and the CPU time was 2 s. Equivalent results were obtained for various set of operating conditions.

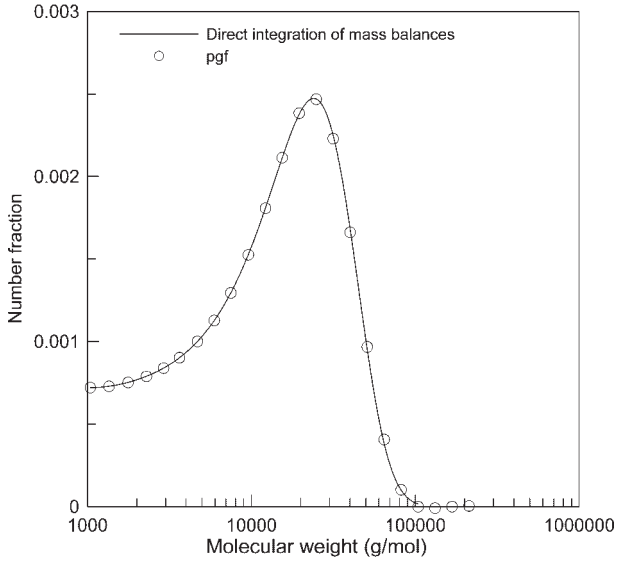

Figure 5. Number fraction of the overall polymer calculated with the pgf technique and by direct integration of the mass balances. Tubular reactor operating conditions: $T = 135\ ^{\circ}C$, $x_{St,inlet} = 0.9976$, $x_{BPO,inlet} = 0.00134$, $x_{TEMPO,inlet} = 0.00106$, $f_{Tot} = 3\ g \cdot min^{-1}$.

As discussed in the section Mathematical model, the kinetic mechanism and model parameters are considered to be reliable since they had already been employed to successfully predict experimental data on batch processes. Besides, results presented above show proper prediction of conversions as well as complete MWDs, polydispersity indexes and average molecular weights obtained from the computed MWDs. Consistency of MWD predictions using either the pgf technique or the direct integration of the mass balances has also been shown. Therefore, the pgf model presented in this work can be considered reliable. Moreover, the advantages of the adjustable model size and reduced computational time are transferred to the solution of optimizations problems. As illustrative examples, two optimization problems were solved that involved finding the operating conditions for obtaining a target MWD. Details follow.

Optimization Examples

As mentioned before, a test of the optimization capabilities of the pgf technique was performed using the two MWD targets shown in Figure 7. The corresponding weight-

Macromol. React. Eng. **2007**, *1*, 622–634

DOI: 10.1002/mren.200700026

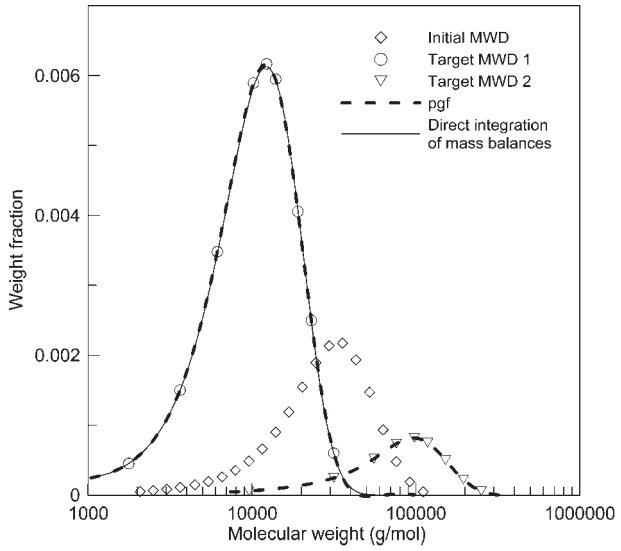

Figure 7. Target, initial, and final MWDs using the pgf method and the direct integration of the mass balances.

average molecular weights are 15 100 and 115 800. Both distributions have a polydispersity index of 1.4.

The initial point for the optimizations was $T = 135\ ^{\circ}C$, $f_{St} = 2.9928\ g \cdot min^{-1}$, $f_{BPO} = 0.00402\ g \cdot min^{-1}$ and $f_{TEMPO} = 0.00318\ g \cdot min^{-1}$. For these operating conditions the MWD is the one shown in Figure 7 as initial MWD. This corresponds to a $\overline{M}_w$ of 43 000 and a polydispersity index of 1.4. The search range chosen for both optimizations was $2\ g \cdot min^{-1} \leq f_{St} \leq 4.5\ g \cdot min^{-1}$, $0.0005\ g \cdot min^{-1} \leq f_{BPO} \leq 0.006\ g \cdot min^{-1}$, $0.0001\ g \cdot min^{-1} \leq f_{TEMPO} \leq 0.005\ g \cdot min^{-1}$, and $100\ ^{\circ}C \leq T \leq 135\ ^{\circ}C$.

When solving the low molecular weight target distribution, the following result was obtained using the pgf technique:

$$f_{St}^{*} = 2\ g \cdot min^{-1}$$
$$f_{BPO}^{*} = 0.00569\ g \cdot min^{-1}$$
$$f_{TEMPO}^{*} = 0.005\ g \cdot min^{-1}$$
$$T^{*} = 134.95\ ^{\circ}C$$

A smaller monomer to TEMPO ratio compared to the initial point is employed to obtain the low MWD, which is expected for this type of polymerization mechanism.[1,13,15] Temperature remains practically unchanged.

The CPU time was 8.5 min with 47 NLP iterations. The final MWD is shown in Figure 7 together with the target MWD. It should be noted that the chain length values relevant for the optimization are only the ones for which the target MWD is given. Therefore, in order to minimize the size of the mathematical model for the optimization, only the nine points indicated with circles in the figure were included in the optimization. This resulted in 540 differential equations related with MWD prediction. Afterwards the optimal point was simulated including more points of the MWD in order to obtain the corresponding curve shown in Figure 7.

For the same target MWD, the optimization result obtained with the direct integration of the mass balances was very similar:

$$f_{St}^{*} = 2\ g \cdot min^{-1}$$
$$f_{BPO}^{*} = 0.00572\ g \cdot min^{-1}$$
$$f_{TEMPO}^{*} = 0.005\ g \cdot min^{-1}$$
$$T^{*} = 134.46\ ^{\circ}C$$

confirming the consistency of the pgf approach. As before, the results for the MWD are shown in Figure 7. As with the pgf case, the size of the mathematical model was reduced as much as possible for the optimization. However, the direct integration of the mass balances approach requires to include all distribution points up to the specified maximum chain length. Therefore, 305 points of the MWD were computed in order to cover the range of the target MWD. This resulted in 915 differential equations. The CPU time for the direct model was 36 min with 58 NLP iterations, which illustrates the considerable benefit of the pgf technique when tailoring the model size to the optimization problem requirements. It is important to observe that the CPU time required for solution of the reduced pgf model was 4.2 times smaller than the CPU time required for solving the model using direct integration of the mass balances.

For the high molecular weight target distribution, the pgf technique afforded the following result:

$$f_{St}^{*} = 2\ g \cdot min^{-1}$$
$$f_{BPO}^{*} = 0.00101\ g \cdot min^{-1}$$
$$f_{TEMPO}^{*} = 0.000868\ g \cdot min^{-1}$$
$$T^{*} = 135\ ^{\circ}C$$

which now involves a larger monomer to TEMPO ratio than in the initial point. The CPU time was 4.7 min with 26 NLP iterations. The final MWD is shown in Figure 7 together with the target MWD. As before, only nine points were included in the model used for the optimization, resulting in the same model size. This was possible because with the pgf technique the number of calculated points can be specified regardless of the particular molecular weight values. Again, extra points were obtained afterwards by simulation.

For the same target MWD, the model size for the direct integration of the mass balances was considerably larger. This was because the MWD had to be computed up to a chain length value of 2 408 in order to cover the range of the target MWD, which resulted in 7 224 differential equations. For this model size, the optimization could not be carried out because of memory overflow on the desktop

computer described before. This is another indication that the proposed optimization scheme using pgf is better suited for optimization purposes.

The optimization solver employed in this work can only guarantee local optimality. However, the excellent agreement between target and final MWDs shown in Figure 7 made further search for global optimality unnecessary.

It is interesting to note the wide range of polymer MWDs that can be potentially achieved with this polymerization setup, and the possibility of using the mathematical tool presented in this work in order to find the required operating conditions.

The approach presented here can be easily applied to other living systems, such as ATRP or RAFT, provided that a kinetic model is available. pgf modeling of the MWD is based on a modular approach. This means that the pgf transform equations of the mass balances of the macromolecular species can be built from the addition of individual pgf transform blocks. These blocks correspond to the transforms of the individual contribution to those mass balances of the different steps of a given kinetic mechanism. The pgf transforms of different variants of individual terms of the mass balances have been tabulated in previous works[19–21] for polymerizations leading to linear or branched polymers. Mass balances resulting from ATRP or RAFT mechanisms have mass balance terms that have the same structure as those included in the mentioned previous works.[19–21] Therefore, application of the pgf approach to these polymerization systems is straightforward.

Conclusion

A mathematical model of the nitroxide-mediated living free radical polymerization in a tubular reactor was presented. The pgf technique was applied for modeling the complete MWD. The model was tested against experimental data, and was successful at predicting conversion, complete MWD, and average properties derived from it.

The average molecular weights calculated from the predicted MWD were in excellent agreement with values obtained by the method of moments. It was also shown that the MWD could be predicted with the same level of accuracy as with those methods that compute the mass balances of all polymeric chains that compose the distribution. At the same time, computational time was much shorter and could be adjusted according to the requirements of different applications. These features make the pgf technique an efficient tool for modeling the complete MWD in simulation and optimization problems.

Work is under way concerning the application of the model for calculating reactor operating and design variables so as to produce polymers with optimal (desired) shapes of their MWD, which involve bimodal and trimodal distributions with specific location of the distribution peaks.

Nomenclature

conv	monomer conversion
I	initiator
C_j	concentration of entity "*j*"
D_n	dormant polymer of chain length *n*
efic	initiator efficiency
f	flow rate
J	parameter of Stehfest inversion algorithm
k_{cap}	kinetic constant of the capping reaction
k_d	kinetic constant of the initiator decomposition reaction
k_{disp1}	kinetic constant of the reaction of disproportionation involving nitroxide
k_p	kinetic constant of the propagation reaction
k_t	kinetic constant of the termination by combination reaction
k_{th}	kinetic constant of the monomer thermal initiation reaction
k_{trm}	kinetic constant of the transfer to monomer reaction
k_{uncap}	kinetic constant of the uncapping reaction
M	styrene monomer
$\overline{M}_n$	number-average molecular weight
$\overline{M}_w$	weight-average molecular weight
M_{BPO}	benzoyl peroxide molecular weight
M_{St}	styrene molecular weight
M_{TEMPO}	TEMPO molecular weight
$n(i)$	predicted value of the number fraction of the overall polymer of chain length *i*
n_i	change length of the *i*th point of the MWD considered in Equation (34)
n_{dist}	number of types of calculated distributions
n_{max}	maximum chain length value of the calculated MWD
n_{points}	number of calculated points of the MWD
n_{spc}	number of different polymeric species for which the pgf transforms are calculated
PDI	polydispersity index
P_n	dead polymer of chain length *n*
r_j	generation rate of entity *j*
R_i	initiation radical
R_n	macroradical of chain length *n*
T	reactor temperature
v	axial velocity
$w(\cdot)$	predicted value of the weight fraction of the overall polymer of chain length indicated between parentheses

Macromol. React. Eng. **2007**, *1*, 622–634

Macromolecular Journals

DOI: 10.1002/mren.200700026

$w_{target}(\cdot)$	desired value of the weight fraction of the overall polymer of chain length indicated between parentheses
x	mass fraction
X	capping agent (TEMPO)
Y	inert species
z	axial distance

Greek Letters

$\delta_{n,a}$	Kronecker delta
$\phi_a(l)$	pgf of the chain length distribution of macroradicals
$\varphi_a(l)$	pgf of the chain length distribution of dormant polymer
λ_a	ath order moment of the chain length distribution of macroradicals
τ	tubular reactor residence time
μ_a	ath order moment of the chain length distribution of the dormant polymer
ρ	density
$\psi_a(l)$	pgf of the chain length distribution of the dead polymer
ζ_a	ath order moment of the chain length distribution of dead polymer
$\vartheta_a(l)$	pgf of the overall polymer (macroradical plus dormant polymer plus dead polymer)

Subscripts

BPO	benzoyl peroxide
inlet	at reactor inlet
max	maximum
min	minimum
mix	reaction mixture
pol	polystyrene
St	styrene
Tot	total

Superscripts

$*$	optimal point

Acknowledgements: The authors wish to thank *CONICET (National Research Council of Argentina), UNS (Universidad Nacional del Sur, Bahía Blanca, Argentina), CAPES (Comitê de Aperfeiçoamento de Pessoal do Ensino Superior), CNPq (Conselho Nacional de Desenvolvimento Científico e Tecnológico, Brazil)* and *NSERC (Natural Sciences and Engineering Research Council of Canada)* for financial support.

Received: June 26, 2007; Revised: August 21, 2007; Accepted: August 22, 2007; DOI: 10.1002/mren.200700026

Keywords: free radical; living polymerization; molecular weight distribution; modeling; probability generating functions

[1] M. Zhang, W. H. J. Ray, *J. Appl. Polym. Sci.* **2002**, *86*, 1630.
[2] K. Matyjaszewski, J. Spanswick, *Mater. Today* **2005**, *8*, 26.
[3] K. Matyjaszewski, J. Xia, *Chem. Rev.* **2001**, *101*, 2921.
[4] W. A. Braunecker, K. Matyjaszewski, *Prog. Polym. Sci.* **2007**, *32*, 93.
[5] A. Goto, T. Fukuda, *Prog. Polym. Sci.* **2004**, *29*, 329.
[6] M. Roa-Luna, A. Nabifar, M. P. Díaz-Barber, N. T. McManus, E. Vivaldo-Lima, L. M. F. Lona, A. Penlidis, *J. Macromol. Sci. Part A-Pure Appl. Chem.* **2007**, *44*, 337.
[7] M. K. Lenzi, M. F. Cunningham, E. L. Lima, J. C. Pinto, *Ind. Eng. Chem. Res.* **2005**, *44*, 2568.
[8] M. Zhang, W. H. J. Ray, *J. Appl. Polym. Sci.* **2002**, *86*, 1047.
[9] H. Chaffey-Millar, M. Busch, T. P. Davis, M. H. Stenzel, C. Barner-Kowollik, *Macromol. Theory Simul.* **2005**, *14*, 143.
[10] J. He, H. Zhang, J. Chen, Y. Yang, *Macromolecules* **1997**, *30*, 8010.
[11] M. K. Lenzi, Ph. D. Thesis, COPPE/UFRJ, Rio de Janeiro 2004.
[12] P. Vana, T. P. Davis, C. Barner-Kowollik, *Macromol. Theory Simul.* **2002**, *11*, 823.
[13] T. M. Kruse, R. Souleimonova, A. Cho, M. K. Gray, J. M. Torkelson, L. J. Broadbelt, *Macromolecules* **2003**, *36*, 7812.
[14] J. Bonilla, E. Saldívar, A. Flores-Tlacuahuac, E. Vivaldo-Lima, R. Pfaendner, F. Tiscareño-Lechuga, *Polym. React. Eng.* **2002**, *10*, 227.
[15] H. Fischer, *J. Polym. Sci. Polym. Chem.* **1999**, *37*, 1885.
[16] R. Lemoine-Nava, A. Flores-Tlacuahuac, *Ind. Eng. Chem. Res.* **2006**, *45*, 4637.
[17] Y. Wang, R. A. Hutchinson, M. F. Cunningham, *Macromol. Mater. Eng.* **2005**, *290*, 230.
[18] M. Wulkow, *Macromol. Theory Simul.* **1996**, *5*, 393.
[19] M. Asteasuain, C. Sarmoria, A. Brandolin, *Polymer* **2002**, *43*, 2513.
[20] M. Asteasuain, A. Brandolin, C. Sarmoria, *Polymer* **2002**, *43*, 2529.
[21] M. Asteasuain, Ph. D. Thesis, Universidad Nacional del Sur, Bahía Blanca 2003.
[22] J. W. Ma, M. F. Cunningham, K. B. McAuley, B. Keoshkerian, M. Georges, *Chem. Eng. Sci.* **2003**, *58*, 1177.
[23] P. A. Cabral, P. A. Melo, E. C. Biscaia, Jr., E. L. Lima, J. C. Pinto, *Polym. Eng. Sci.* **2003**, *43*, 1163.
[24] M. P. Vega, E. L. Lima, J. C. Pinto, *Comput. Chem. Eng.* **1997**, *21*, S1049.
[25] M. D. Saban, M. K. Georges, R. P. N. Veregin, G. K. Hamer, P. M. Kazmaier, *Macromolecules* **1995**, *28*, 7032.

[26] A. Brandolin, M. Asteasuain, C. Sarmoria, A. R. López, K. S. Whiteley, B. del Amo Fernández, *Polym. Eng. Sci.* **2001**, *41*, 1156.
[27] M. Asteasuain, M. V. Pérez, C. Sarmoria, A. Brandolin, *Latin Am. Appl. Res.* **2003**, *33*, 241.
[28] M. Asteasuain, C. Sarmoria, A. Brandolin, *J. Appl. Polym. Sci.* **2003**, *88*, 1676.
[29] M. Asteasuain, A. Brandolin, C. Sarmoria, *Polymer* **2004**, *45*, 321.
[30] M. Asteasuain, A. Brandolin, *J. Appl. Polym. Sci.* **2007**, *105*, 2621.
[31] Process Systems Enterprise, Ltd., *"gPROMS v2.3.1 Introductory User Guide"*, 2005.
[32] R. P. N. Veregin, P. G. Odell, L. M. Michalak, M. K. Georges, *Macromolecules* **1996**, *29*, 3346.
[33] R. P. N. Veregin, P. G. Odell, L. M. Michalak, M. K. Georges, *Macromolecules* **1996**, *29*, 2746.
[34] P. B. Zetterlund, Y. Saka, R. McHale, T. Nakamura, F. Aldabbagh, M. Okubo, *Polymer* **2006**, *47*, 7900.
[35] J. C. Pinto, A. Vianna, Jr., E. Biscaia, Jr., *Polym. Eng. Sci.*, in press.

DOI: 10.1002/mren.200700026